Experimental Study on the Design of a Refrigeration System Based on a Small-scale Centrifugal Compressor with Gas Foil Bearings [#]

Xiang Qiu [1], Jingyang Hua [1], Chenyi Qian [1], Jiaxuan Wang [1], Binbin Yu [1*], Junye Shi [1,2], Jiangping Chen [1,3*]

1 Institute of Refrigeration and Cryogenics, Shanghai Jiao Tong University, Shanghai 200240, China

2 Shanghai Jiao Tong University ZhongGuanCun Research Institute, Liyang 213300, China

3 Shanghai Engineering Research Center of High Efficient Cooling System, Shanghai, 200240, China
*Corresponding Author: E-mail: ybbedc@sjtu.edu.cn; jpchen_sjtu@163.com

ABSTRACT

Small-scale centrifugal compressors have the potential to offer higher efficiency and operate without oil, compared to positive displacement compressors. With advancements in industrial design and manufacturing technology, the potential for replacing traditional positive displacement compressors with small-scale centrifugal compressors is increasing. While centrifugal compressors have traditionally been favored for large systems with cooling capacities of several hundred kilowatts or more, their application in smaller refrigeration systems, with capacities in the tens of kilowatts, has not been thoroughly explored and remains under-researched. In this study, a 45 kW refrigeration system test bench was constructed using an R134a small-scale oil-free centrifugal compressor with gas foil bearings. The experiment investigated the impact of key design factors, including refrigerant charge amount and *the* settings *of* air-cooled condenser fan, on system performance. After optimization, the system achieved a maximum cooling capacity of 44.54 kW and a highest COP of 3.59 under design conditions (ambient temperature of 35°C). Additionally, control strategies for cooling service were designed and main control parameters were calibrated, with experimental results indicating that the system successfully performed cooling tasks and operated with stable parameters.

Keywords: Vapor compression refrigeration cycle, Small-scale centrifugal compressor, System design, System performance, Air-cooled condenser, Control strategies

NONMENCLATURE

Abbreviations	
c	Specific heat capacity, kJ/(kg·K)
COP	Coefficient of performance

EEV	Electronic expansion valve
GWP	Global warming potential
IIR	International Institute of Refrigeration
$\dot{m}$	Mass flow rate, kg/s
Q_c	Cooling capacity, kW
RPM	Revolutions per minute
t	Time, s
T	Temperature, ℃
T_a	Real-time coolant temperature, ℃
T_t	User-defined set point, ℃
V	Volumetric flow rate, m3/s
W	Power consumption, kW
Greek symbols	
ρ	Density of fluid, kg/m
Subscripts	
com	Compressor
fan	Condenser fan
i	Inlet condition
o	Outlet condition
pump	Circulation pump

1. INTRODUCTION

As the global energy crisis intensifies and environmental concerns escalate, there is unprecedented societal focus on energy conservation and emission reduction. The International Institute of Refrigeration (IIR) estimates that around 5 billion refrigeration, air conditioning, and heat pump systems are in operation worldwide, contributing to global annual sales of approximately 500 billion USD. The refrigeration sector accounts for about 20% of the world total electricity consumption [1]. Therefore, improving the energy efficiency of refrigeration equipment is a key strategy for mitigating the energy crisis and addressing environmental challenges.

In applications with moderate cooling capacity requirements (less than 50 kW), traditional positive displacement compressors are commonly used [2]. However, these compressors face challenges such as lower efficiency compared to centrifugal refrigeration units and issues related to oil operation. This study is motivated by the potential of small-scale centrifugal compressors to offer higher efficiency than the currently used positive displacement compressors [3]. Additionally, their ability for oil-free operation provides significant advantages in advanced refrigeration cycle system design, enhancing heat transfer performance in both the evaporator and condenser [4, 5]. Furthermore, centrifugal compressors can operate at very high speeds, allowing for significant size reduction while maintaining performance [3]. This capability enables integration with advanced heat exchangers [6], facilitating the design of compact and lightweight cooling systems that are especially suitable for applications with strict space and weight constraints [7, 8].

The development of small-scale oil-free centrifugal compressors, known for their compact size, simple structure, and high flow rate, has become a major focus of research [9]. This trend supports the advancement of small cooling capacity refrigeration systems based on centrifugal compressors. Two primary technological pathways are being explored for this development. One approach involves magnetic bearings, which offer advantages such as high speed, efficiency, and reduced noise but require complex control systems and are associated with high costs [10, 11]. The alternative approach uses gas foil bearings, which, in addition to being high-speed and oil-free, feature a simpler structure, flexible bearing installation, cost-effectiveness, and do not require active control [12, 13]. In addition, advances in air compressors for fuel cell systems have significantly matured the technology for small-scale, oil-free centrifugal compressors [14]. Building on this progress, the current research applies this technology to the development of small-scale, oil-free refrigeration centrifugal compressors.

In the past few years, scholars have conducted extensive research on centrifugal compressor refrigeration systems, with research mainly focusing on systems with large cooling capacity (more than 100 kW). These researches mainly concentrated on improving system energy efficiency [15-18], and optimizing centrifugal compressor design [19-24].

However, research on small-scale oil-free refrigeration centrifugal compressors is limited. J. Schiffmann et al. [4, 25] developed a multi-objective optimization approach for high-efficiency, low-power compressors for domestic heat pumps, ensuring efficiency across a wide range. Giuffre et al. [26] optimized a two-stage compressor for aircraft environmental control systems, achieving over 70% efficiency and a compression ratio above 9. Mechanical Solutions, Inc. [27] created an ultra-small centrifugal compressor with the low GWP refrigerant R515A, which Lennox International, Inc. tested, showing cooling capacities of 1.5 to 2.9 TR and efficiency between 55% and 60%. M. V. Casey et al. [28] used dimensional analysis to scale down centrifugal compressors, aligning motor power with compressor needs. M.N. Šarevski et al. [29] explored effects of high impeller speeds on flow characteristics. Darene Essa et al. [30] modeled an electric vehicle cooling system with ultrahigh-speed micro compressors, finding HFC-134a had the best cooling capacity and power consumption. Adeel Javed et al. [31] designed a 6.5 kW heat pump with two small-scale centrifugal compressors, highlighting challenges in managing tip leakage flow. V.N. Šarevski et al. [32] developed a compact centrifugal compressor with oil-free bearings and R134a, achieving a pressure ratio of 3.3 and over 78% efficiency at 210 krpm.

In summary, research on small-scale oil-free centrifugal compressors mainly focuses on optimizing compressor design and limited experimentation. Comprehensive studies on the cycle characteristics and performance of these systems are still lacking. This study makes a significant contribution by establishing a 45 kW refrigeration system test bench using a small-scale oil-free centrifugal compressor with gas foil bearings. Experimental investigations were conducted to investigate the effects of refrigerant charge amount and air-cooled condenser settings on system performance, and to test the system optimized performance under designed condition. Finally, the study involved calibrating the system main control parameters based on the control strategy.

2. EXPERIMENTAL SETUP

2.1 Experimental setup description

Fig. 1 illustrates the schematic diagram of the experimental setup of the refrigeration system based on a small-scale oil-free two-stage centrifugal compressor. The system consists of a core loop (refrigerant loop) and an auxiliary loop (coolant loop). The refrigerant loop consists of a compressor, a plate evaporator, an air-cooled condenser, an electronic expansion valve (EEV), and a liquid reservoir. However, what sets it apart is the
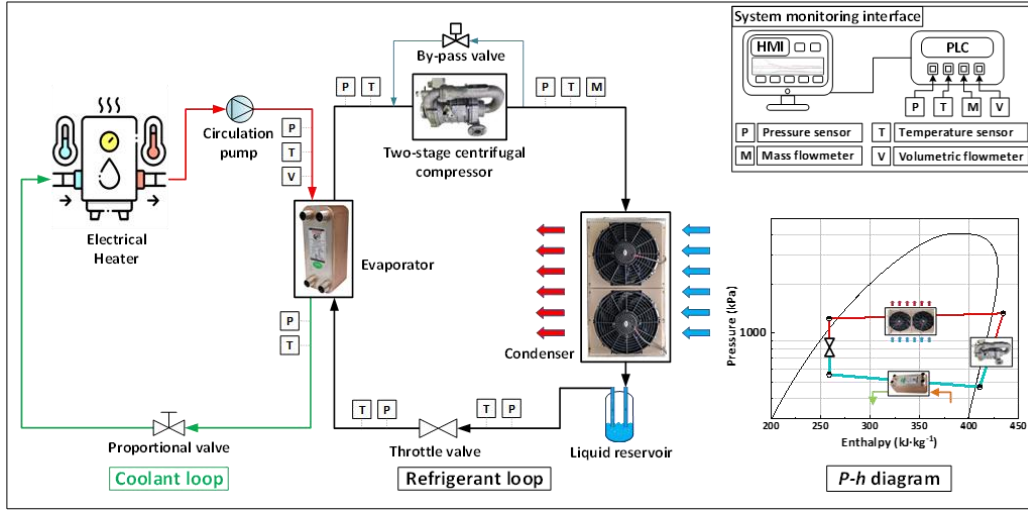
Fig. 1 Schematic diagram of the experimental setup and measuring points

utilization of a centrifugal compressor in the system designed for a cooling capacity of 45 kW. Traditionally, centrifugal compressors have been deemed inappropriate for cooling capacities of this scale [33]. And this study aims to demonstrate the competitiveness of centrifugal compressors in cooling scenarios of this scale by leveraging a small-scale oil-free centrifugal compressor developed based on gas foil bearing technology. It should be noted that, to address potential surge issues in the centrifugal compressor, the system is equipped with a bypass valve parallel to the compressor. The coolant loop includes an electric heater, circulation pump, and a proportional valve. Adjusting the power of electric heater controls the inlet temperature of the coolant entering the evaporator. Circulation pump drives this loop, while the proportional valve regulates the coolant flow rate. Additionally, the specifications for the main components used in the system are detailed in Table 1.

Fig. 2 depicts the shape and dimensions of the small-scale oil-free refrigeration centrifugal compressor, designed with a cooling capacity of 45 kW. The compressor has an outer profile length of 280 mm and an outer diameter of 160 mm, while its inner profile measures 170 mm in length and 120 mm in inner diameter. It features a compact design, significantly smaller than a scroll compressor of comparable cooling capacity. The compressor adopts advanced foil gas bearings technology, which, in addition to being high-speed and oil-free, features a simpler structure, versatile bearing installation, cost-effectiveness, and the added advantage of not requiring active control. Combined with high-speed motor technology, the compressor can achieve speeds of up to 120,000 rpm, enabling it to achieve 45 kW cooling capacity with such a small size.

Furthermore, the application of gas foil bearing technology brings the additional benefit of being oil-free. This simplifies the system structure by eliminating the need for a lubrication oil circuit and also offers advantages for heat exchangers, as lubricating oil would reduce heat transfer efficiency [33].

Table 1 Specifications of experimental equipment.

Component	Specification
Compressor	Type: Two-stage centrifugal compressor
	Maximum speed: 120,000 rpm
	Designed pressure ratio and mass flow rate: 2.93, 0.307 kg/s
	Type of bearing: Gas foil bearing
	Type of motor: Permanent Magnet Synchronous Motor (PMSM)
	Refrigerant: R134a
	Rated voltage: 400V DC
Evaporator	Type: Brazed plate heat exchangers
	Size(mm): 192(L)×217(W)×617(H)
	Materials: AISI 316
Condenser	Type: Counterflow microchannel heat exchanger
	Size(mm):1400(L)×950(W)
	Number of flat tubes: 138
	Specifications of flat tubes: 32×2-18
	Material grade of flat tubes:3F03+Zn-H112
	Fin specifications:32×0.08 FPI=21
	Refrigerant flow path: 55/41/27/15
Fan	Rated voltage: 400V AC
	Frequency:50/69 Hz
	Maximum speed：1870 rpm
	Maximum back pressure：500Pa
Valve	Control steps: 0-500 steps
	Rated voltage: 12V, DC
Circulation pump	Rated flow rate: 20 m³/h
	Rated head: 22m
Electrical heater	Maximum heating power: 80kW

2.2 Data reduction

The system cooling capacity (Q_c) is defined as the cooling capacity on the coolant side and can be calculated using Eq. (1).
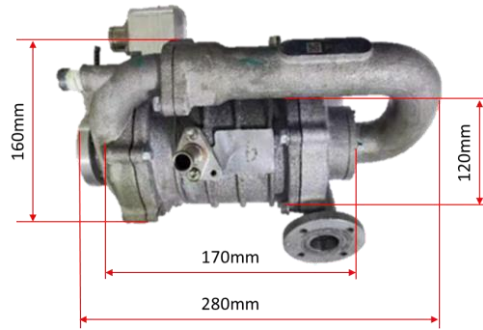
$$Q_c = c\rho V(T_i - T_o) \qquad (1)$$

Fig. 2 Dimensions of Small-scale oil-free refrigeration centrifugal compressor with 45 kW cooling capacity

where c is the specific heat capacity of the coolant (Ethylene Glycol 50/50) in kJ/(kg· K), ρ is the density of coolant in kg/m³, V is the volumetric flow rate of the coolant in m³/s, T_{in} is the inlet temperature of the coolant in the evaporator (℃), T_{out} is the outlet temperature of the coolant in the evaporator (℃).

The system coefficient of performance (COP) of the refrigeration system is calculated using Eq. (2).

$$COP = \frac{Q_c}{W_{com} + W_{pump} + W_{fan}} \qquad (2)$$

Where W_{com} is the compressor power consumption in kW, W_{pump} is the coolant circulation pump power consumption in kW, W_{fan} is air-cooled condenser fan power consumption in kW. These power consumptions are directly measured using a digital power meter.

2.3 Test method and test conditions

The study first determined the appropriate refrigerant charge amount through experiments. It then investigated the impact of condenser fan settings on system performance, including factors such as the distance between the fan and the condenser heat exchange core and the fan speed. Following this, the performance of the optimized system was tested under design conditions (35℃ ambient temperature). Finally, a control strategy for the system cooling application was developed, and key control parameters were experimentally calibrated, including an additional fitting function for the optimal fan speed in relation to compressor speed and ambient temperature. Specific test conditions for each experiment are detailed in Table 2.

Table 2 Experimental test conditions.

No.	Compressor Speed (krpm)	Fan speed (rpm)	Coolant Flow rate (L/min)	Coolant temperature (℃)	Ambient temperature(℃)
#1	110	1800	320	18	40
#2	110	1200	320	18	40
#3	110	1200-1800	320	18	40
#4	30-115	/	320	18	35

3. EXPERIMENTAL RESULTS AND DISCUSSION

3.1 Determining the amount of refrigerant charge

For the vapor compression refrigeration system, its performance is significantly affected by the refrigerant charge amount. If the charge amount of refrigerant is insufficient, the system performance declines. This study first determines the appropriate charge amount for the system under test condition #1.

Fig. 3 shows how cooling capacity, compressor power consumption, and system COP change with variations in refrigerant charge amount. As the charge amount increases from 6 kg to 7 kg, cooling capacity rises from 37.81 kW to 40.31 kW, and compressor power consumption increases from 8.09 kW to 8.63 kW. The COP, which reflects the efficiency of cooling relative to power consumption, improves from 3.10 to 3.17. Importantly, once the charge amount exceeds 6.6 kg, there is minimal additional increase in cooling capacity, compressor power consumption, or system COP, suggesting that the charge amount has reached a plateau. To account for potential refrigerant leakage and ensure stable performance, the optimal charge amount should exceed this plateau entry point. Thus, for this study, a charge amount of 7.0 kg was chosen for the subsequent experiments.

3.2 Determining the settings of air-cooled condenser fan

The settings of air-cooled condenser fans significantly affects the performance of the refrigeration system. If the distance between the fan and the heat exchange core is either too far or too close, it results in poor heat dissipation. Moreover, too short a distance increases the fans power consumption. Low fan speed leads to insufficient condenser heat dissipation, limiting system performance; whereas high fan speed does not significantly improve system performance but dramatically increases the fan's power consumption, reducing system efficiency. This section investigates the
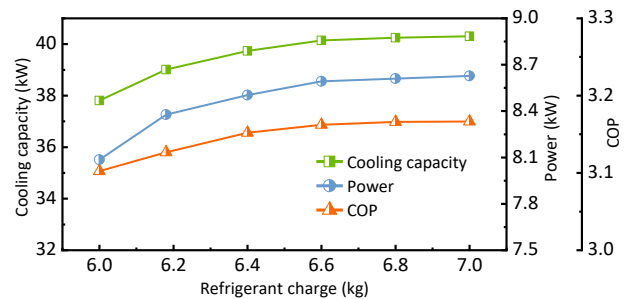

Fig. 3 Variations of cooling capacity, compressor power consumption, and system COP under different refrigerant charge amount

impact of the distance between the fan and the condenser heat exchange core, as well as the fan speed, on system performance under test condition #2 and #3.

Fig. 4(a) illustrates the variations in cooling capacity, system power consumption, and system COP with the change in the distance between the fan and the heat exchange core. As the distance increases from 100 mm to 150 mm, the cooling capacity increases rapidly from 37.76 kW to 40.12 kW, beyond this distance, the cooling capacity decreases. This is because a short distance causes uneven airflow distribution, while a large distance results in insufficient airflow, both of which weaken the condenser heat dissipation capacity, reducing system cooling capacity. Increasing the distance reduces fan resistance and, consequently, fan power consumption, resulting in a decrease in system power consumption from 13.69 kW at 100 mm to 12.09 kW at 250 mm. Up to 150 mm, the cooling capacity increases while power consumption decreases, significantly improving the system COP. After 150 mm, although the cooling capacity declines, the power consumption also significantly decreases, slightly improving the system COP. Considering the compactness of the system spatial arrangement, a distance of 150 mm was selected.

Fig. 4(b) and Fig. 4(c) depict the changes in cooling capacity, system COP, as well as system power consumption, compressor power consumption, and fan power consumption with varying fan speeds. As the fan speed increases from 1200 rpm to 1800 rpm, the system cooling capacity rises from 40.4 kW to 41.7 kW, due to the increased heat dissipation capacity of the condenser. The system COP initially increases and then decreases, reaching a maximum value of 3.18 at 1500 rpm, and rapidly declining beyond 1600 rpm. This is because, beyond 1500 rpm, the rate of increase in cooling capacity slows, while fan power consumption continues to rise sharply, leading to a noticeable increase in total system power consumption after 1600 rpm. Therefore, in the design of air-cooled condenser refrigeration systems,

selecting an appropriate fan speed is crucial for optimizing system performance.

3.3 System performance and effects of compressor speed

After determining the refrigerant charge amount and air-cooled condenser fan settings, experiments tested the performance of the optimized system at various compressor speeds under design conditions (ambient temperature of 35°C). It is essential to note that the speed of the centrifugal compressor is crucial to system operation, directly affecting system performance. Studying the impact of compressor speed on system characteristics is also an integral part of system design. Experiments were conducted under operating condition #4, with the EEV opening and fan speed adjusted in real-time to ensure maximum system COP at each compressor speed.

Fig .5 shows how cooling capacity, compressor power consumption, and system COP vary with changes in compressor speed. As the compressor speed increases, cooling capacity exhibits a nonlinear trend: it gradually increases from 3.16 kW to 10.72 kW as speed rises from 30 krpm to 70 krpm. Beyond 70 krpm, cooling capacity sharply increases to 44.54 kW at 115 krpm, accounting for 81.7% of the total variation in cooling capacity. Compressor power consumption follows a similar trend, with a rapid increase continuing even past 110 krpm. It is important to note that the nonlinear variation in system characteristics caused by changes in compressor speed is highly significant, particularly in system design, and especially crucial for the design of control systems. The system reaches its maximum cooling capacity of 44.54 kW at 115 krpm. The peak system COP of 3.59 is achieved at a compressor speed of 90 krpm, where the increase in cooling capacity before 90 krpm outweighs the rise in compressor power consumption. However, after this point, the rapid
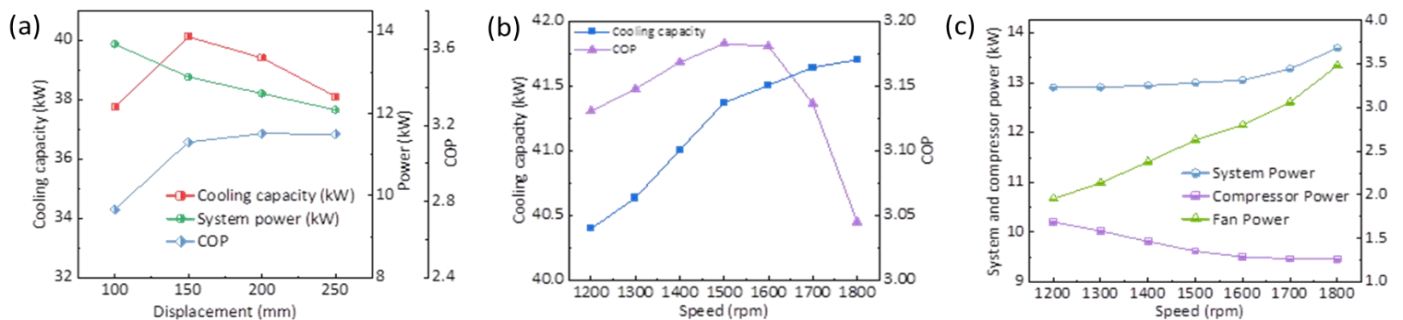

Fig. 4 Effect of air-cooled condenser fan settings on system performance. (a) Distance between the fan and the heat exchange core. (b)(c) Condenser fan speed.
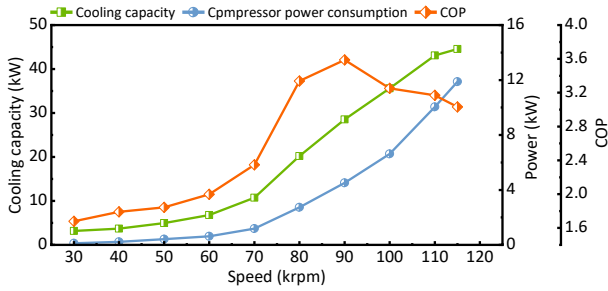
Fig. 5 Variations of cooling capacity, compressor power consumption, and system COP under different compressor speed

increase in power consumption outpaces the cooling capacity gain, causing a decline in system COP.

3.4 Calibration of the system control strategy

The final step in the system design is to determine the control strategy and calibrate the main control parameters. The system is used to provide cooling services to other equipment, ensuring that the coolant temperature does not exceed $T_t + 2$ ℃ (where T_t is the user-defined set point).

Fig. 6 illustrates the specific control strategy. After the unit starts, it first automatically initializes and continuously monitors the coolant temperature T_a. If $T_a > T_t + 2$, the unit is activated. During startup, the fan and electronic expansion valve are activated t_1 seconds before the compressor to provide conditions for a smooth compressor start. The compressor speed, fan speed, and electronic expansion valve steps are stabilized at preset values for t_2 seconds in the startup phase. Subsequently, the system enters the automatic control phase, where the compressor, fan, electronic expansion valve, and pump are controlled according to calibrated PID parameters. During this phase, the system continuously monitors for any occurrence of surge (If the power fluctuates more than 7 % (a value based on our engineering experience) above the average power in three consecutive readings, indicating a surge condition). If surge occurs, surge prevention measures are implemented, such as increasing fan speed or opening the bypass valve. If the surge is resolved, the system resumes automatic control until $T_a < T_t + 2$, after which it enters the exit cooling program and returns to standby status. If the surge continues, the system will directly enter the exit cooling procedure. If surge occurs three times in succession, the system will shut down, and engineers need to check the system.

As discussed in Section 3.2, appropriate fan speed is crucial for ensuring system performance. It is evident that as compressor speed increases, the condenser heat

dissipation requirements grow; Similarly, higher ambient temperatures make heat dissipation more challenging. Both scenarios require higher fan speeds to provide greater airflow. We have previously noted that excessively high fan speeds result in minimal performance improvement but significantly increased power consumption, reducing system efficiency. To achieve optimal system performance (the highest system COP), we investigated the effects of ambient temperature and compressor speed on the optimal fan speed through experimental studies. A binary function was used to fit the measurement data, with an R^2 value greater than 0.95. The fitting results are shown in Fig. 7. Subsequent studies used this fitting formula to control fan speed. For compressor speed, electronic expansion
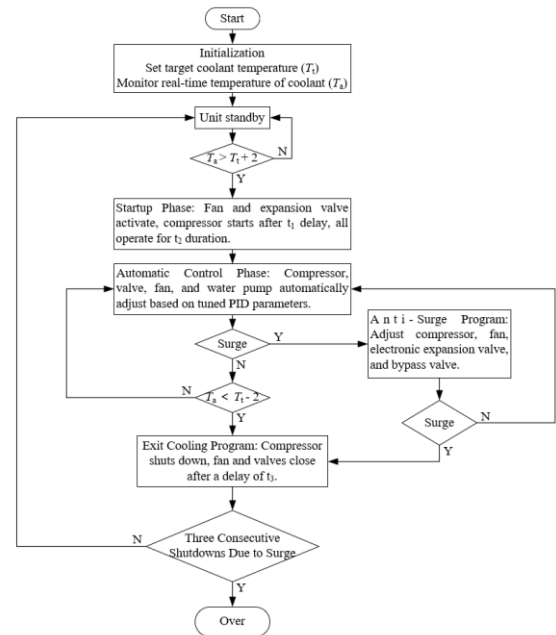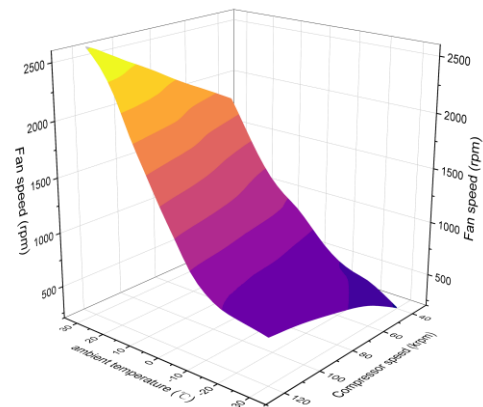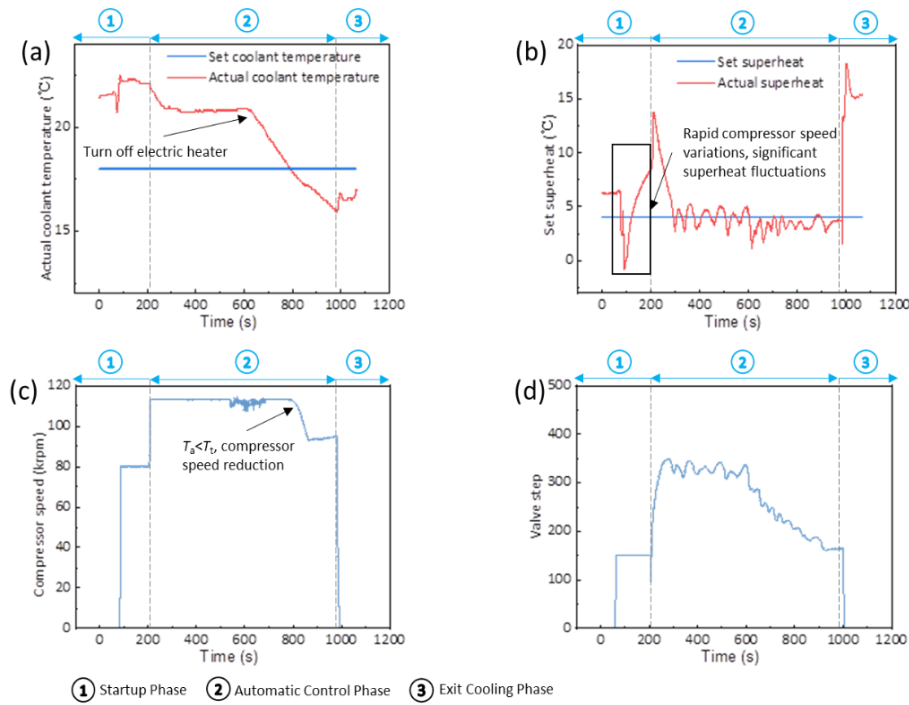

Fig. 6 Control strategies for cooling services

Fig. 7 Fitting diagram of optimal fan speed with respect to ambient temperature and compressor speed

Fig. 8 System operation after calibrating control parameters. (a)(c) Coolant temperature and corresponding compressor speed variations. (b)(d) Evaporator outlet superheat and corresponding electronic expansion valve steps

valve, and water pump, control parameters were calibrated according to classical control theory[34].

Take the system operation results at 35 ℃ ambient temperature as an example, the system control strategy calibration results are shown in Fig. 8, where Fig. 8(a) and Fig. 8(c) represent the coolant temperature and corresponding compressor speed variations, and Fig. 8(b) and Fig. 8(d) show the evaporator outlet superheat and corresponding electronic expansion valve step changes. The experiment simulated two scenarios: $T_a>T_t+2$ (unit activation) and $T_a<T_t-2$ (unit shutdown). When $T_a>T_t+2$, the unit enters the startup phase. During this phase, the compressor speed is preset to 80 krpm, resulting in a lower cooling capacity but stabilizing the cooling fluid temperature. The electronic expansion valve step is preset to 150, and the superheat fluctuates greatly due to the sudden change of the system status. After entering the automatic control phase, the system calculates the control parameters of compressor, electronic expansion valve and pump according to the calibrated PID parameters. During the transition from startup phase to automatic control phase, the compressor speed rapidly increases to its maximum value while the coolant temperature quickly decreases and then stabilizes. The sudden increase in compressor speed causes the suction superheat to rapidly rise to around 15°C. To maintain a reasonable superheat, the electronic expansion valve step increases rapidly, with superheat decreasing to around 4°C and then fluctuated

slightly. Later in this phase, the heater is turned off, causing a continuous decrease in coolant temperature. When $T_a<T_t$, the compressor speed begins to decrease but remains above 90 krpm. The electronic expansion valve also responds promptly, reducing its opening to maintain superheat around 4°C. After $T_a<T_t-2$, the system enters the exit cooling program. The control program successfully completed the cooling service, keeping all system parameters within the acceptable range.

4.   CONCLUSIONS

This study established a 45 kW refrigeration system test bench based on an R134a small-scale oil-free centrifugal compressor with gas foil bearings. It experimentally investigated the effects of key system design parameters, such as refrigerant charge amount and air-cooled condenser fan configuration, on system performance. The study also explored the system performance variation of the optimized system with compressor speed under design conditions (ambient temperature of 35°C). Finally, it developed control strategies for cooling applications and calibrated critical control parameters. The main conclusions are as follows:

1.   A refrigerant charge amount of 7.0 kg is considered appropriate for the system, balancing performance and efficiency while allowing for system stability.

2.   For air-cooled condensers, a distance between the fan and the condenser heat exchange core that is

too small results in uneven airflow distribution, while a distance that is too large leads to insufficient airflow. This study determined that the optimal distance is 150 mm. Additionally, selecting an appropriate fan speed is critical for maintaining system performance. Low fan speed leads to inadequate condenser heat dissipation, whereas high fan speed provides only minimal performance improvement but significantly increases power consumption, thus reducing system efficiency.

3. Under design conditions (ambient temperature of 35°C), the system can operate stably with compressor speeds ranging from 30 to 115 krpm, with no surge detected. The system reaches its maximum cooling capacity of 44.54 kW at 115 krpm. The peak system COP of 3.59 is achieved at a compressor speed of 90 krpm,

4. Calibration results show that the system can successfully complete the cooling service and maintain all parameters within acceptable levels, based on the designed control strategy and calibrated control parameters.

REFERENCE

[1] L. DJ. The Role of Refrigeration in the Global Economy (2019), 38th Note on Refrigeration Technologies. International Institute of Refrigeration (IIR) 2019.

[2] Guoyuan M, Qiuyu S, Yuexuan G, Xiaoya J, Shuxue X. Evaluation on the state-ofart and future trend for minitype refrigerant compressor. Refrigeration and Air-Conditioning. 2022;22(03):63-71.

[3] Gresh MT. Chapter 1 - Introduction to Aerodynamics. In: Gresh MT, editor. Compressor Performance (Third Edition): Butterworth-Heinemann; 2018. p. 3-11.

[4] Schiffmann J, Favrat D. Design, experimental investigation and multi-objective optimization of a small-scale radial compressor for heat pump applications. Energy. 2010;35(1):436-50.

[5] Yu FW, Chan KT, Sit RKY, Yang J. Performance Evaluation of Oil-free Chillers for Building Energy Performance Improvement. Procedia Engineering. 2015;121:975-83.

[6] Qian C, Wang J, Zhong H, Qiu X, Yu B, Shi J, et al. Experimental investigation on heat transfer characteristics of copper heat exchangers based on triply periodic minimal surfaces (TPMS). International Communications in Heat and Mass Transfer. 2024;152:107292.

[7] Wang J, Yu B, Qian C, Shi J, Chen J. Experimental study on the boiling heat transfer characteristics of a pump-driven two-phase cooling loop system for high heat flux avionics. Thermal Science and Engineering Progress. 2023;45:102150.

[8] Zhao C, Mazo JR, Verstraete D. Optimisation of a liquid cooling system for eVTOL aircraft: Impact of sizing mission and battery size. Applied Thermal Engineering. 2024;246:122988.

[9] Song J, Liu G, Gong J, Yang Q, Zhao Y, Li L. Simulation on performance and regulation strategy of centrifugal refrigeration compressor with gas bearings in water chiller. Applied Thermal Engineering. 2024;236:121650.

[10] Rejith R, Kesavan D, Chakravarthy P, Narayana Murty SVS. Bearings for aerospace applications. Tribology International. 2023;181:108312.

[11] Siva Srinivas R, Tiwari R, Kannababu C. Application of active magnetic bearings in flexible rotordynamic systems – A state-of-the-art review. Mechanical Systems and Signal Processing. 2018;106:537-72.

[12] Shi T, Wang H, Yang W, Peng X. Mathematical modeling and optimization of gas foil bearings-rotor system in hydrogen fuel cell vehicles. Energy. 2024;290:130129.

[13] Shi T, Zhang J, Peng X, Feng J, Guo Y, Wang B. Startup optimization of gas foil bearings-rotor system in proton exchange membrane fuel cells. Journal of Cleaner Production. 2024;436:140594.

[14] Wu Y, Bao H, Fu J, Wang X, Liu J. Review of recent developments in fuel cell centrifugal air compressor: Comprehensive performance and testing techniques. International Journal of Hydrogen Energy. 2023;48(82):32039-55.

[15] Deymi-Dashtebayaz M, Farahnak M, Abadi RNB. Energy saving and environmental impact of optimizing the number of condenser fans in centrifugal chillers under partial load operation. International Journal of Refrigeration. 2019;103:163-79.

[16] Deng J, Qiang W, Peng C, Wei Q, Zhang H. Research on systematic analysis and optimization method for chillers based on model predictive control: A case study. Energy and Buildings. 2023;285:112916.

[17] Lyu W, Wang Z, Li X, Xin X, Chen S, Yang Y, et al. Energy efficiency and economic analysis of utilizing

magnetic bearing chillers for the cooling of data centers. Journal of Building Engineering. 2022;48:103920.

[18] Liu H, Zhao B, Zhang Z, Li H, Hu B, Wang RZ. Experimental validation of an advanced heat pump system with high-efficiency centrifugal compressor. Energy. 2020;213:118968.

[19] Tang X, Gu N, Wang W, Wang Z, Peng R. Aerodynamic robustness optimization and design exploration of centrifugal compressor impeller under uncertainties. International Journal of Heat and Mass Transfer. 2021;180:121799.

[20] Hosseinimaab SM, Tousi AM. Optimizing the performance of a single-shaft micro gas turbine engine by modifying its centrifugal compressor design. Energy Conversion and Management. 2022;271:116245.

[21] Ekradi K, Madadi A. Performance improvement of a transonic centrifugal compressor impeller with splitter blade by three-dimensional optimization. Energy. 2020;201:117582.

[22] Romei A, Gaetani P, Persico G. Computational fluid-dynamic investigation of a centrifugal compressor with inlet guide vanes for supercritical carbon dioxide power systems. Energy. 2022;255:124469.

[23] Jiao K, Sun H, Li X, Wu H, Krivitzky E, Schram T, et al. Numerical simulation of air flow through turbocharger compressors with dual volute design. Applied Energy. 2009;86(11):2494-506.

[24] He Y, Chen H, Xu Y, Deng J. Compression performance optimization considering variable charge pressure in an adiabatic compressed air energy storage system. Energy. 2018;165:349-59.

[25] Schiffmann J, Favrat D. Experimental investigation of a direct driven radial compressor for domestic heat pumps. International Journal of Refrigeration. 2009;32(8):1918-28.

[26] Giuffre A, Colonna P, Pini M. Design Optimization of a High-Speed Twin-Stage Compressor for Next-Gen Aircraft Environmental Control System. Journal of Engineering for Gas Turbines and Power. 2022;145(3).

[27] Bouza A, Payne J, Bennett E. Low-GWP HVAC System with Ultra-small Centrifugal Compression. Mechanical Solutions, Inc.; 2018.

[28] Casey M, Krähenbuhl D, Zwyssig C. The design of ultra-high-speed miniature centrifugal compressors. Conference The design of ultra-high-speed miniature centrifugal compressors. EUROPEAN TURBOMACHINERY SOCIETY.

[29] Šarevski MN, Šarevski VN. Characteristics of water vapor turbocompressors applied in refrigeration and heat pump systems. International Journal of Refrigeration. 2012;35(5):1484-96.

[30] Essa D, Spickler B, Depcik C, Shiflett MB. Air conditioning cycle simulations using a ultrahigh-speed centrifugal compressor for electric vehicle applications. International Journal of Refrigeration. 2021;131:803-16.

[31] Javed A, Arpagaus C, Bertsch S, Schiffmann J. Small-scale turbocompressors for wide-range operation with large tip-clearances for a two-stage heat pump concept. International Journal of Refrigeration. 2016;69:285-302.

[32] Šarevski VN, Šarevski MN. Energy efficiency of the thermocompression refrigerating and heat pump systems. International Journal of Refrigeration. 2012;35(4):1067-79.

[33] Hundy GF, Trott AR, Welch TC. Chapter 4 - Compressors. In: Hundy GF, Trott AR, Welch TC, editors. Refrigeration, Air Conditioning and Heat Pumps (Fifth Edition): Butterworth-Heinemann; 2016. p. 59-87.

[34] O'Dwyer A. Controller tuning rules for non-self-regulating process models. Handbook of PI and PID controller tuning rules 3rd ed. London: Imperial College Press; 2009.